Chapter 4

Ratcheting Fatigue Behaviour of Inconel 617 alloy at RT

4.1 Introduction

This chapter presents the ratcheting fatigue behaviour of Inconel 617 alloy under asymmetrical stress control cyclic loading and the effect of various parameters such as mean stress, stress amplitude and stress rate on fatigue life. Also, a comparison has been made with the ratcheting behaviour of modified 9Cr-1Mo steel with the help of normalized mean stress and stress amplitude at constant stress rate at room temperature. Similar studies have been conducted on nickel based superalloys by several researchers. Kong et al.,(2022) studied uniaxial ratcheting fatigue behaviour and fracture mechanism of GH742 superalloy at 650^{o}C. The results highlight that the fatigue life significantly decreases with increasing mean stress or stress amplitude. The alloy initially exhibits a cyclic hardening response, followed by cyclic softening until fracture under asymmetric cyclic loading. Similarly Liu et al.,(2019) studied ratcheting fatigue of the nickel based superalloy GH4169 at 650^{o}C.The results show that a distinct reduction in fatigue life occurs with the increase in mean stress and stress amplitude. A continuous cyclic softening until final failure is observed for all the tests.

Inconel 617 alloy is primarily used as piping/tubing material in power generating industries. The chapter includes microstructural characterization of the Inconel 617 alloy in the heat-treated condition. Tensile properties of the alloy were evaluated at a strain rate of 10^{-3} s^{-1}, at room temperature. The parameters used for studying ratcheting behaviour are stress amplitude, mean stress and stress rate. Fatigue tests were carried out under uniaxial asymmetric cyclic stress with maximum stress (σ_{max}),in the region close to yield strength (YS) and also in the region of ultimate tensile strength (UTS) of the material.The range of the three variables was: stress amplitude (225 to 600 MPa), mean stress (150 to 250 MPa), and stress rate (50 to 450 MPa/s). Ratcheting fatigue experiments were performed on MTS-810 servo-hydraulic fatigue testing system of 50 kN load capacity.

When one parameter such as mean stress was varied, other two parameters such as stress amplitude and stress rate were maintained at constant level. Characterization of fracture features was performed using scanning electron microscopy. TEM analysis of tested samples showed variation in dislocation substructures developed under the different variables.

4.2 Microstructural characterization of Inconel 617 alloy

The solutionizing treatment cycle involves heating the Inconel 617 alloy to 1175^{o}C and exposing it for a period of time (40 minutes in the present case), determined by the cross section size of the alloy, followed by quenching in water.

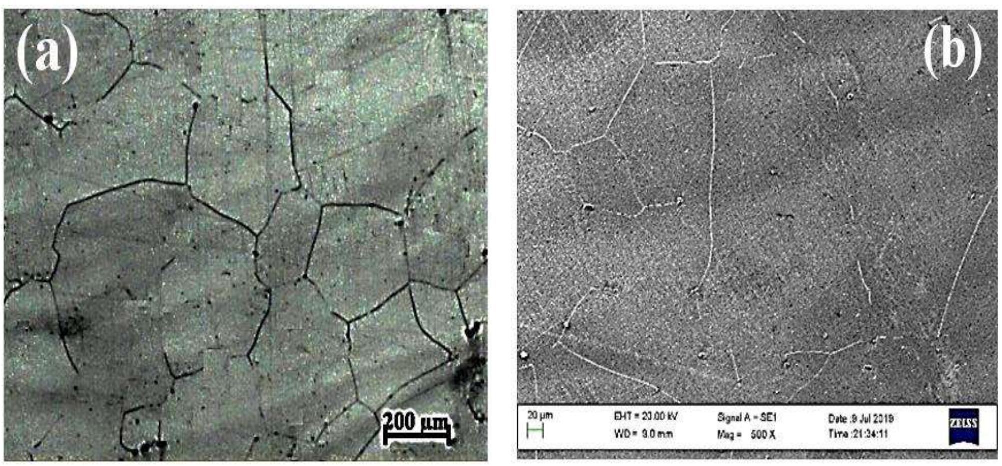

Fig. 4.1 Microstructure of the Inconel 617 alloy in solution treated (1175^{o}C/40 min/WQ) condition: (a) optical micrograph showing single phase matrix (γ) and (b) SEM micrograph showing $M_{23}C_6$ carbide particles along grain boundaries.

Fig. 4.1(a) displays microstructure of the solution treated Inconel 617 alloy showing single phase austenitic matrix. The mean intercept length of the grains was found to be 100 µm. Fig. 4.1(b) shows SEM micrograph depicting $M_{23}C_6$ carbides along some grain boundaries. No precipitates were observed within the grains. This microstructure is similar to that reported by others in solution treated condition [Rao et al., (2019)].

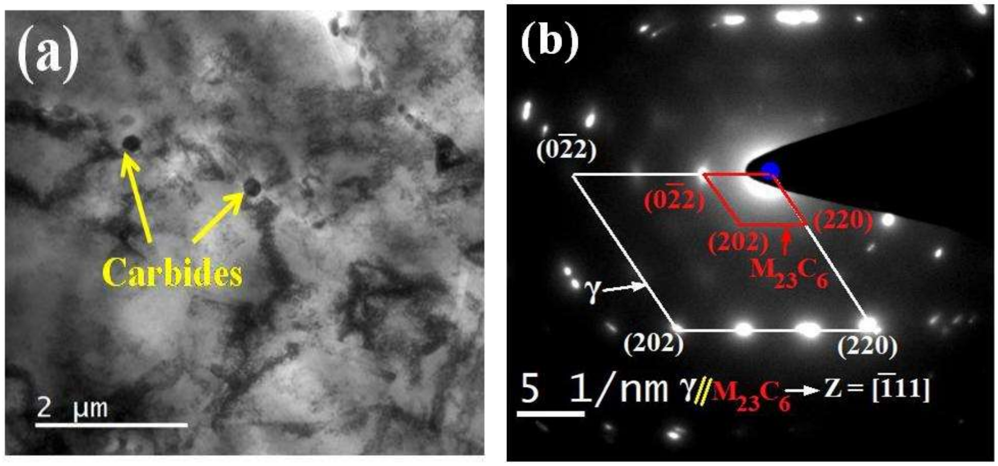

Fig. 4.2 Bright field TEM micrographs of the Inconel 617 alloy in solution treated condition showing: (a) $M_{23}C_6$ carbide particles along grain boundaries and (b) Diffraction pattern confirming precipitates of $M_{23}C_6$ carbide (*fcc*) with cube on cube orientation relationship with the matrix (*fcc*).

TEM micrographs of the Inconel 617 alloy in solution treated condition in Fig. 4.2(a) shows precipitates along the grain boundary. The diffraction pattern corresponding to precipitate is shown in Fig. 4.2(b), that confirms the presence of fine precipitates of $M_{23}C_6$ carbide (lattice parameter, a: 10.6Å) along the grain boundaries of the γ matrix (lattice parameter, a: 3.608 Å). The average size of the $M_{23}C_6$ carbide precipitates lies between 400-1000 nm. The precipitates appear to be semi-coherent

4.3 Tensile properties of Inconel 617 alloy

The tensile engineering stress-strain curve of the Inconel 617 alloy in the solution treated condition, corresponding to strain rate of 10^{-3} s^{-1} is displayed in Fig. 4.3, and the tensile properties are listed in Table 4.1. The matrix for the ratcheting fatigue tests was formed based on the YS and UTS of the material and maximum stress was taken above the value of YS and below the value of UTS.

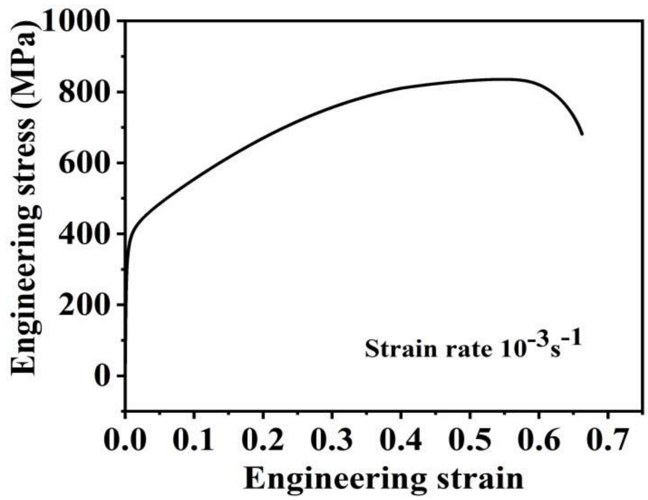

Fig .4.3 Engineering stress-strain curve of Inconel 617 alloy.

Table 4.1 Strength and ductility parameters of the Inconel 617 alloy tested, at the strain rate of 10^{-3} s $^{-1}$, at RT.

0.2% Yield Strength (MPa)	Ultimate Tensile Strength (MPa)	Elongation (%)	Uniform plastic elongation (%)	Reduction in area (%)	Strength coefficient (K) (MPa)	Strain hardening exponent (n)	Degree of work hardening (S_{UTS}/S_{YS})
347	835	66	54	68	1578	0.36	2.41

4.4 Uniaxial ratcheting fatigue behaviour of Inconel 617 alloy

Uniaxial ratcheting fatigue behaviour of the Inconel 617 alloy, under asymmetric cyclic loading, was studied varying the mean stress, stress amplitude and stress rate. It may be seen that there is a large difference of about 488 MPa between the yield strength and ultimate tensile strength of the material. Therefore, a few interrupted tests were conducted with the maximum stress near the yield strength, some tests with maximum stress in the intermediate region of the YS and UTS, and one test was conducted at the maximum stress close to the tensile strength, to analyse the ratcheting as well as fracture behaviour in different regions of the applied cyclic stress.

4.4.1 Effect of the stress amplitude on cyclic response of Inconel 617 alloy under asymmetric cyclic loading

(a) ***Fatigue tests performed with the maximum stress near the yield strength***

Hysteresis loops of the samples tested up to 200 cycles, under asymmetric cyclic loading with mean stress of 200 MPa, stress amplitude of 450 MPa and stress rate of 150 MPa/s, are displayed in Fig. 4.4(a).

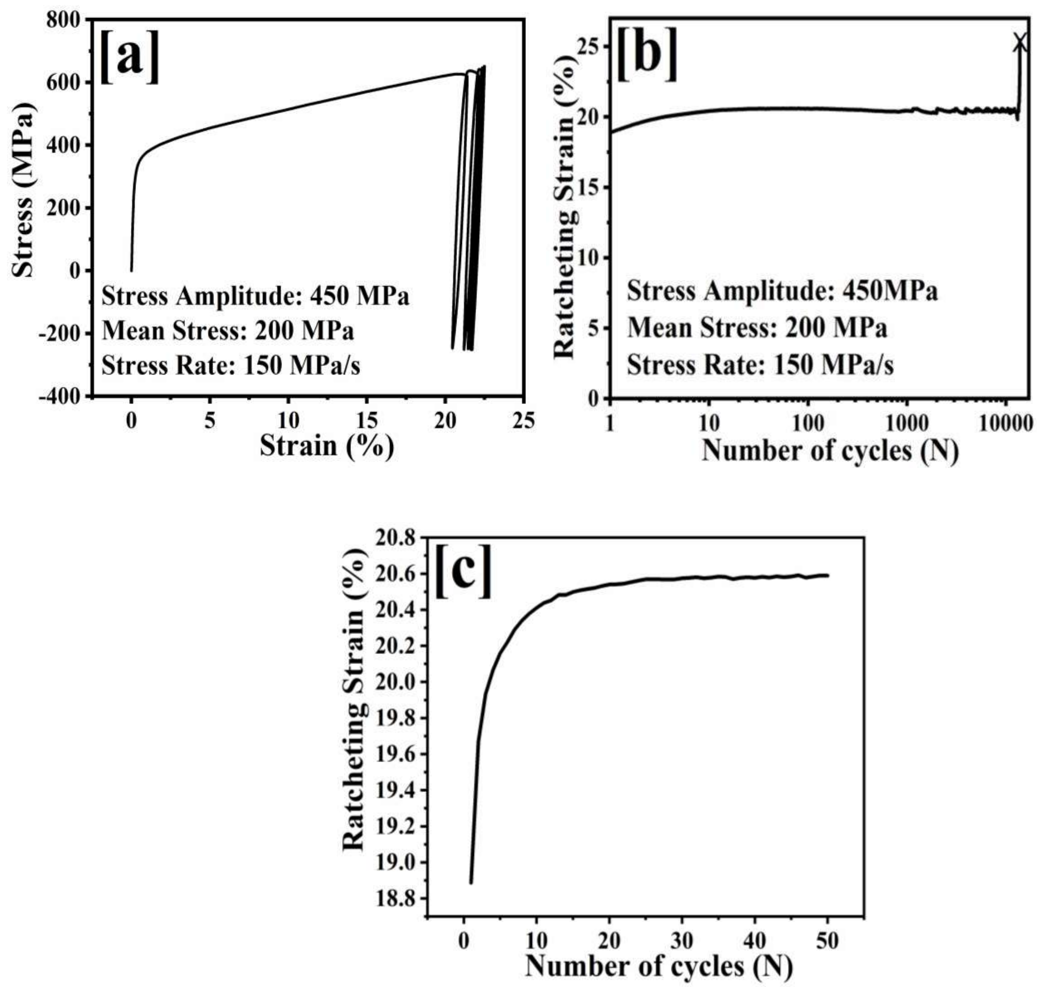

Fig. 4.4 Ratcheting fatigue behaviour of Inconel 617 alloy during asymmetric cyclic loading: (a) drastic decrease in loop width after 1st cycle (b) variation of ratcheting strain with cycles till fracture and (c) increase in ratcheting strain during the initial 50 cycles.

The applied maximum stress (σ_{max}) and minimum stress (σ_{min}) was 650 MPa and 250 MPa, respectively. The 1st cycle shows maximum accumulation of the permanent strain. As the loading is asymmetric, the loops may be seen to be partially closed in the beginning; however, the extent of non-closure continuously decreases with increase in cycles, as depicted in Fig. 4.4(a). The shifting of loops towards right side led to progressive increase in the tensile permanent deformation. In the beginning, up to about 20 cycles, the accumulation of ratcheting strain is very fast, as seen from the magnified view (Fig. 4.4c); however, the increase in the ratcheting strain is almost negligible, during the intermediate region till about 12000 cycles; after that, there is very fast increase till fracture (Fig. 4.4b).

Table 4.2 Test matrix of ratcheting fatigue tests of Inconel 617 alloy at varying stress amplitude, at constant mean stress of 200 MPa and stress rate of 150 MPa/s.

S.No.	Maximum stress (σ_{max}) MPa	Minimum stress (σ_{min}) MPa	Mean stress (σ_m) MPa	Stress amplitude (σ_a) MPa	Stress rate ($\dot{\sigma}$) MPa/s	Interrupted at cycles
1	425	-25	200	**225**	150	**1000**
2	450	-50	200	**250**	150	**1000**
3	475	-75	200	**275**	150	**1000**
4	500	-100	200	**300**	150	**1000**

Four tests conducted at low stress amplitude of 225 to 300 MPa, were interrupted at 1000 cycles, as they would take long time to fracture. Three tests were conducted in the intermediate region of the YS (347 MPa) and UTS (835 MPa); at stress amplitude of 450, 500 and 550 MPa, mean stress of 150, 200 and 250 MPa and stress rate of 50,150 and 450 MPa/s at the respective maximum stress values (σ_{max} of 650, 700 and 750 MPa). These tests were carried out till fracture.

One test was conducted at the highest stress amplitude of 600 MPa, at corresponding maximum stress of 800 MPa, near UTS of the material, till fracture. Table 4.2 shows the matrix of asymmetric fatigue tests carried out at varying stress amplitudes of 225, 250, 275 and 300 MPa, which were interrupted at 1000 cycles.

Fig. 4.5(a) shows ratcheting fatigue behaviour at varying stress amplitudes. It is observed that with increase in stress amplitude, ratcheting strain accumulation increases. During the initial cycles, up to less than 30 cycles, the accumulation of plastic strain is very high. With increase in amplitude from 225 to 300 MPa, strain in the first cycle is increased from 0.6% to 9 %, however, after that it remained constant.

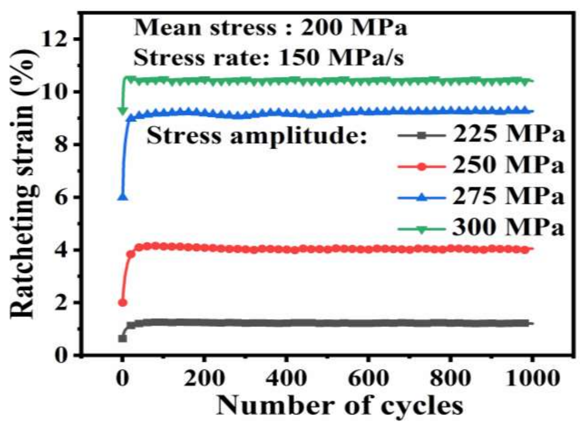

Fig. 4.5 Effect of stress amplitude on ratcheting strain variation with cycles of Inconel 617 alloy.

(b)Fatigue tests at stress amplitude of 450 to 550 MPa with maximum stress of 650 to 750 MPa, in the intermediate region between the YS and UTS

Some tests were performed till fracture for observing the effect of stress amplitude on ratcheting strain accumulation and cyclic life of the material. The test matrix with variation in stress amplitude from 450 to 550 MPa, at constant mean stress of 200 MPa and stress rateof 150 MPa/s is shown in Table 4.3. Cyclic life decreases with increase in stress amplitude from 450 to 550 MPa. It can be observed from Fig. 4.6(a) that accumulation of ratcheting strain increases with increase in the amplitude of stress. The increase in ratcheting strain for the first cycle is from 18.88 to 35.63% with rise in stress amplitude from 450 to 550 MPa, consequently fatigue life is reduced from 13850 to 3104 cycles, (Table 4.3). However, there is not any observable impact of stress amplitude on the rate of ratcheting strain accumulation, as shown in Fig. 4.6(b).

Table 4.3 Variation in fatigue life of Inconel 617 alloy under ratcheting fatigue, at varying stress amplitude, at constant mean stress of 200 MPa and stress rate of 150 MPa/s.

S.No.	Maximum stress (σ_{max}) MPa	Minimum stress (σ_{min}) MPa	Stress amplitude (σ_a) MPa	No. of cycles to failure (N_f)
1	650	-250	**450**	13850
2	700	-300	**500**	8905
3	750	-350	**550**	3104

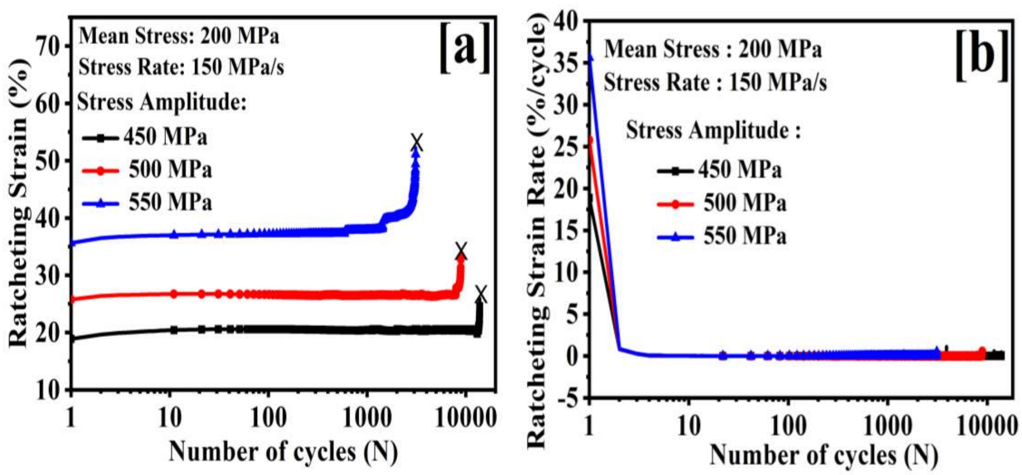

Fig. 4.6 Effect of stress amplitude on ratcheting fatigue of Inconel 617 alloy: (a) variation of ratcheting strain with cycles at different stress amplitudes and (b) rate of accumulation of ratcheting strain with cycles.

(c)Fatigue test with maximum stress near ultimate tensile strength

One test was conducted at the maximum stress level of 800 MPa, close to UTS (835 MPa), at stress amplitude of 600 MPa, mean stress of 200 MPa and stress rate of 150 MPa/s, to study ratcheting fatigue behaviour at high stress level. Since this test was conducted at the highest maximum stress, close to UTS, it lasted only for 43 cycles. The accumulation of strain and the rate of accumulation of strain, resulting from asymmetric cyclic stressing is shown in Figs. 4.7(a and b), respectively. Fig. 4.7(c) shows the fractured fatigue specimen with necking. Also, some unique features and roughness may be seen on the surface in the gauge section, developed due to discontinuous and progressive increase in the accumulated ratcheting strain from cyclic loading.

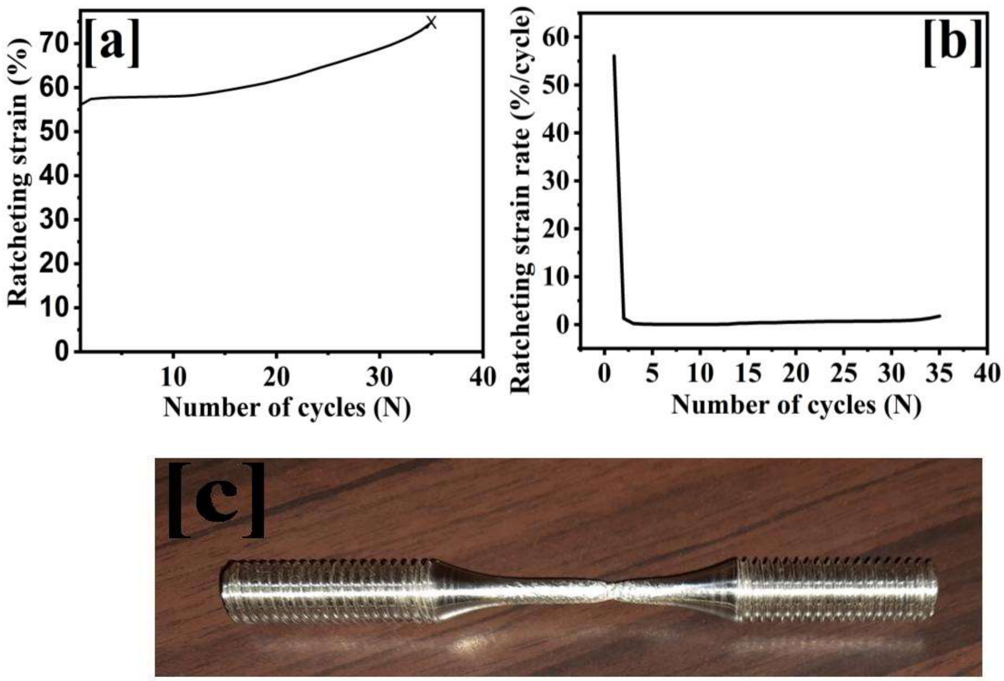

Fig. 4.7 Ratcheting fatigue behaviour of Inconel 617 alloy tested at the stress amplitude close to UTS; stress amplitude of 600 MPa, mean stress of 200 MPa and stress rate of 150 MPa/s: (a) rapid increase in ratcheting strain in the beginning, followed by much slower increase up to about 12 cycles, and rapid increase till fracture (b) variation of ratcheting strain rate with cycles and (c) fractured fatigue specimen showing necking and some scratchy features on surface in the gauge section.

4.4.2 Effect of mean stress on cyclic response of Inconel 617 alloy under asymmetric cyclic loading

Asymmetric load controlled cyclic tests were conducted for studying the influence of positive mean stress on ratcheting strain and cyclic life. The test matrix with maximum and minimum stress was designed in such a way that there is variation in the mean stress from 150 to 250 MPa, while keeping the stress amplitude and stress rate constant, at 500 MPa and 150 MPa/s respectively, (Table 4.4).

Table 4.4 Variation in fatigue life of Inconel 617 alloy under ratcheting fatigue, at varying mean stress and at constant stress amplitude of 500 MPa and stress rate of 150 MPa/s.

S.No.	Maximum stress (σ_{max}) MPa	Minimum stress (σ_{min}) MPa	Mean stress (σ_m) MPa	No. of cycles to failure (N_f)
1	650	-350	**150**	10007
2	700	-300	**200**	8905
3	750	-250	**250**	4206

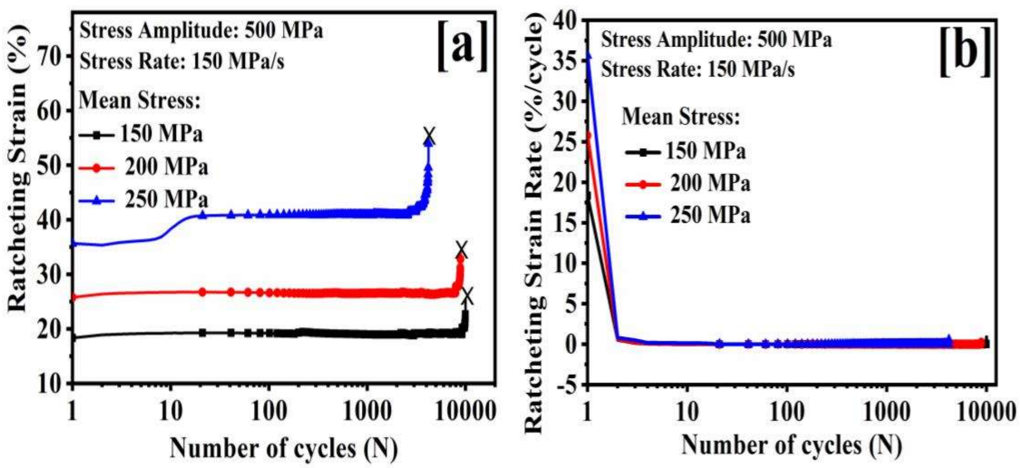

Fig. 4.8 Effect of mean stress on ratcheting fatigue of Inconel 617 alloy: (a) variation of ratcheting strain with cycles under various mean stresses and (b) rate of accumulation of ratcheting strain with cycles.

It may also be observed that as the mean stress increases from 150 to 250 MPa, cyclic life decreases from 10007 to 4206 cycles. Fig. 4.8(a) shows the change in the ratcheting strain accumulation with cycles, up to failure (N_f), at varying mean stress. The ratcheting strain accumulation for the first cycle increases from 18.35% to 35.65%, with increase in the mean stress from 150 to 250 MPa and fatigue life is decreased. The rate of accumulation of ratcheting strain was highest in the beginning and decreased up to about 20 cycles, there after remained nearly constant (Fig. 4.8 b). Two competitive processes, cyclic work hardening and geometrical softening, affect the engineering stress/load control ratcheting.

In the initial stage, when the material is soft and dislocation density is low, large plastic deformation occurs during the initial cycles, however, the rate of accumulation of plastic strain decreases with increase in number of cycles due to cyclic work hardening.

However, softening effect increases due to increase in length and decrease in cross sectional area. Due to balance effect between the cyclic hardening and cyclic softening, the secondary stage occurs after about 20 cycles, and the rate of accumulation of ratcheting strain remains constant. In the second stage also dislocations are arranged in more stable form. In the tertiary stage, reduction in cross sectional area becomes substantial, as in case of modified 9Cr-1Mo steel because of high ratcheting strain accumulation, and hence softening dominates. In the case of low accumulation of ratcheting strain as in Inconel 617 alloy, the tertiary stage of the ratcheting curve occurs due to initiation of fatigue crack.

4.4.3 Effect of stress rate on cyclic response of Inconel 617 alloy under asymmetric cyclic loading

The tests for the third group were performed till fracture for observing the effect of stress rate on ratcheting strain accumulation and fatigue life of the material. The test matrix with variation in stress rate from 50 to 450 MPa/s at constant mean stress of 200 MPa and stress amplitude of 500 MPa/s is shown in Table 4.5.

Table 4.5 Variation in fatigue life of Inconel 617 alloy under ratcheting fatigue at varying stress rate, at constant mean stress of 200 MPa and stress amplitude of 500 MPa.

S.No.	Maximum stress (σ_{max}) MPa	Minimum stress (σ_{min}) MPa	Stress rate ($\dot{\sigma}$) MPa/s	No. of cycles to failure (N_f)
1	700	-300	**50**	4632
2	700	-300	**150**	8905
3	700	-300	**450**	9290

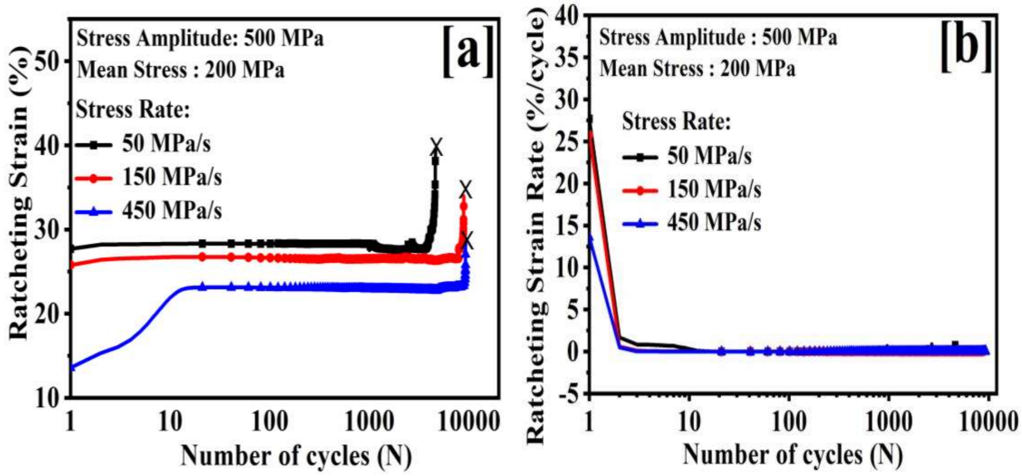

Fig. 4.9 Effect of stress rate on ratcheting fatigue of Inconel 617 alloy: (a) variation of ratcheting strain with cycles under various stress rates and (b) rate of accumulation of ratcheting strain with cycles.

A different type of behaviour, stress rate varying from 50 to 450 MPa/s; at constant mean stress 200 MPa and stress amplitude of 500 MPa, was observed in comparison with those of the stress amplitude and mean stress tests. The cyclic life was found to increase with increase in the stress rate from 50 to 450 MPa/s. It is evident from Fig. 4.9(a) that ratcheting strain accumulation decreases with increase in stress rate. The decrease in ratcheting strain for the first cycle is from 27.7 to 13.6% with rise in stress rate from 50 to 450 MPa/s, consequently fatigue life is enhanced from 4632 to 9290 cycles (Table 4.5). The rate of accumulation of plastic strain also decreases with rise in the stress rate, as shown in Fig. 4.9 (b).

4.5 Cyclic stress-strain behaviour of Inconel 617 alloy

On asymmetrical cyclic stressing, the alloy may exhibit cyclic hardening/softening or cyclically stable behaviour, depending upon the parameters. It can be explained with the help of cyclic stress- strain hysteresis loops. The width or the area of the loops depicts whether the alloy is exhibiting cyclic hardening or softening behaviour.

4.5.1 Impact of stress amplitude on stress-strain behaviour of Inconel 617 alloy under asymmetric cyclic stressing

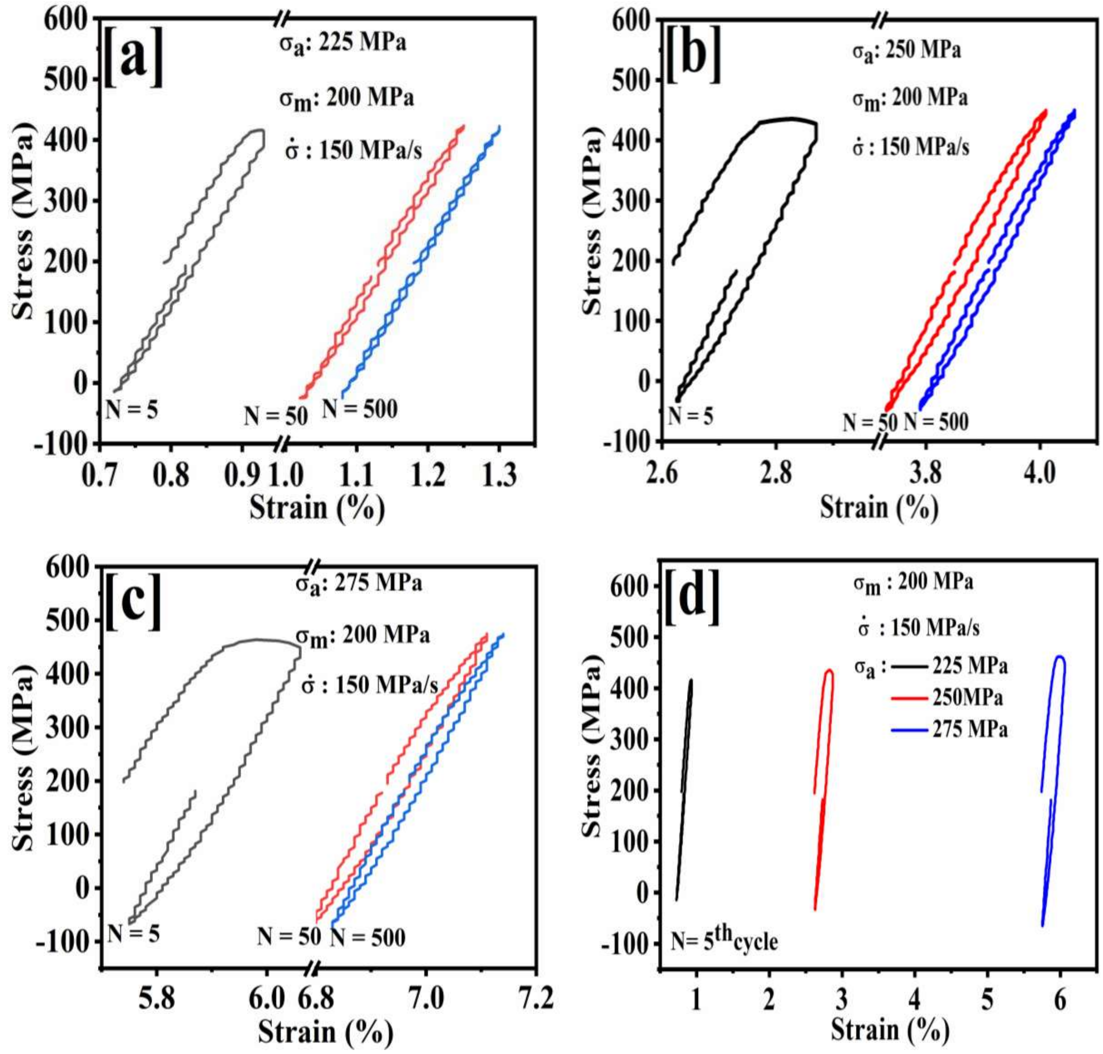

Fig. 4.10 Hysteresis loops of Inconel 617 alloy corresponding to 5, 50 and 500 stress cycles at various stress amplitudes: (a) 225 MPa (b) 250 MPa (c) 275 MPa and (d) comparison of width of the 5th cycle loop at various stress amplitudes, at constant mean stress of 200 MPa and stress rate of 150 MPa/s.

Keeping a particular combination of the three variables, comparison was made of the hysteresis loops in terms of their width at different number of cycles. In general, larger the width of the hysteresis loop, higher is the extent of softening and decrease in the width of the loops signifies increase in cyclic hardening of the material. It may be noticed from Figs. 4.10(a, b and c) that with increase in number of cycles, the width of hysteresis loop decreases; thus, there is increase in hardening of the material with increase in cyclic stressing. Fig. 4.10(d) shows increase in loop width and area with increase in stress amplitude for 5th cycle, thereby exhibiting higher plastic deformation. This can also be correlated with plastic strain energy plot as depicted in Fig. 4.11 that shows decrease in plastic strain energy with increase in number of cycles for a particular value of stress amplitude parameter, and also exhibits increase in plastic strain energy with increase in number of cycles.

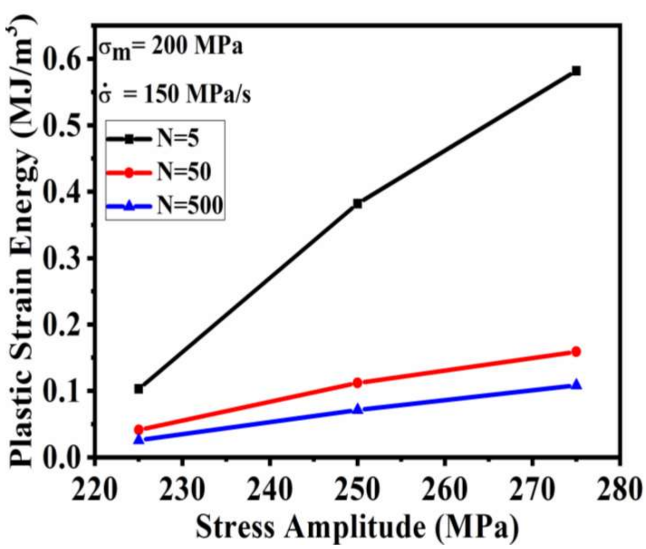

Fig. 4.11 Effect of stress amplitude on hysteresis loop energy of Inconel 617 alloy**,** at different number of cycles at constant mean stress of 200 MPa and stress rate of 150 MPa/s.

4.5.2 Impact of mean stress on stress-strain behaviour of Inconel 617 alloy under asymmetric cyclic stressing

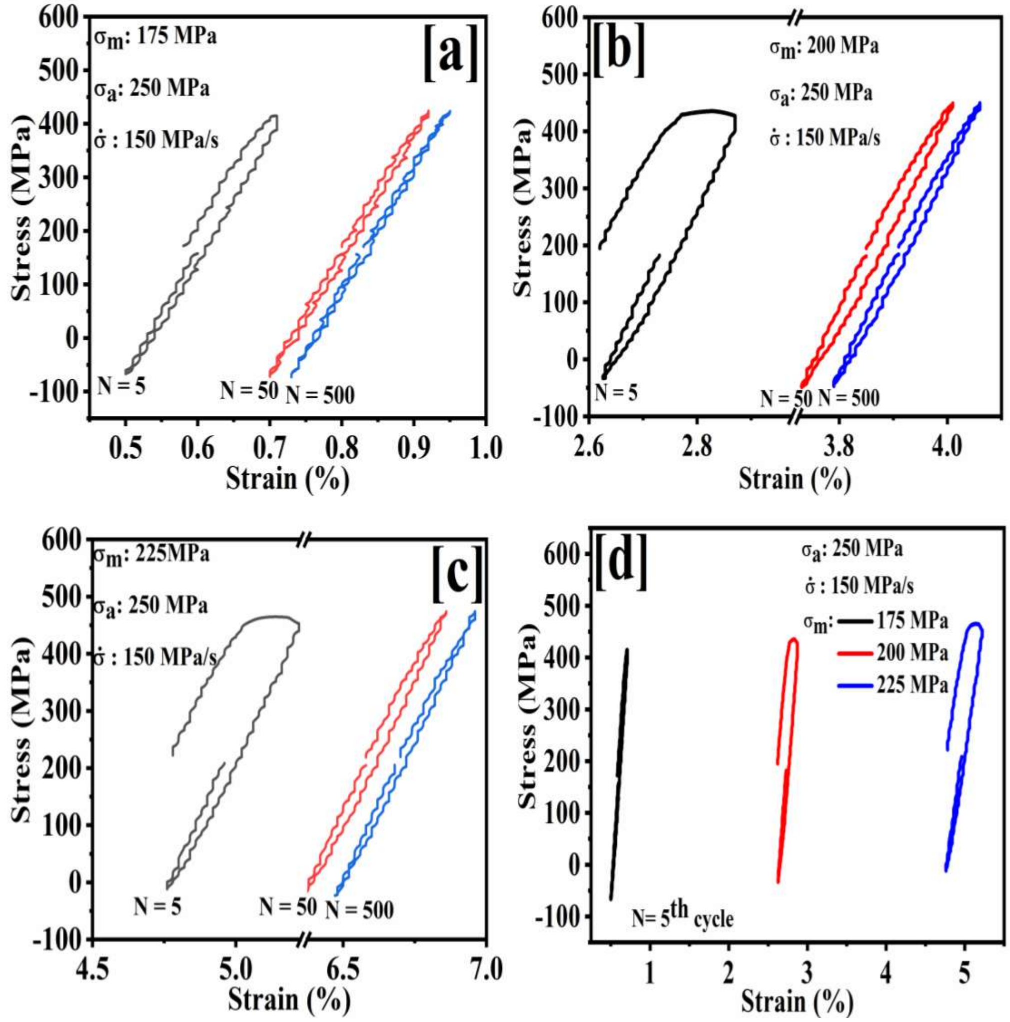

Fig. 4.12 Hysteresis loops of Inconel 617 alloy corresponding to 5, 50 and 500 stress cycles at various mean stresses: (a) 175 MPa, (b) 200 MPa, (c) 225 MPa and (d) comparison of width of 5th cycle loop at various mean stresses, at constant stress amplitude of 250 MPa and stress rate of 150 MPa/s.

In Fig. 4.12 the effect of mean stress from 175-225 MPa, at constant stress amplitude of 250 MPa and stress rate of 150 MPa/s, is presented at 5, 50 and 500 cycles. The general rule is that more the hysteresis loop area, more amount of energy is absorbed by the material and this lowers the fatigue life.

It may be very well visualized from Figs. 4.12(a, b and c) that for a particular mean stress with increase in number of cycles, the width of hysteresis loop decreases, which means that with increase in number of cycles the material exhibits cyclic hardening. Fig. 4.12(d) depicts hysteresis loop at various mean stresses for 5th cycle. It shows increase in loop width with increase in mean stress and that is attributed to higher plastic deformation of the material.

The plastic strain energy plot (Fig. 4.13) shows that with increase in the number of cycles, for a particular mean stress, plastic strain energy decreases but with increase in mean stress, it first increases and then decreases; it means that at the highest mean stress of 225 MPa, the material exhibits hardening behaviour which can also be correlated with the loops (Figs. 4.12 b and c) at mean stresses of 200 MPa and 225 MPa. The reason behind the hardening behaviour has been very well explained along with microstructural characterization in the discussion section of this chapter.

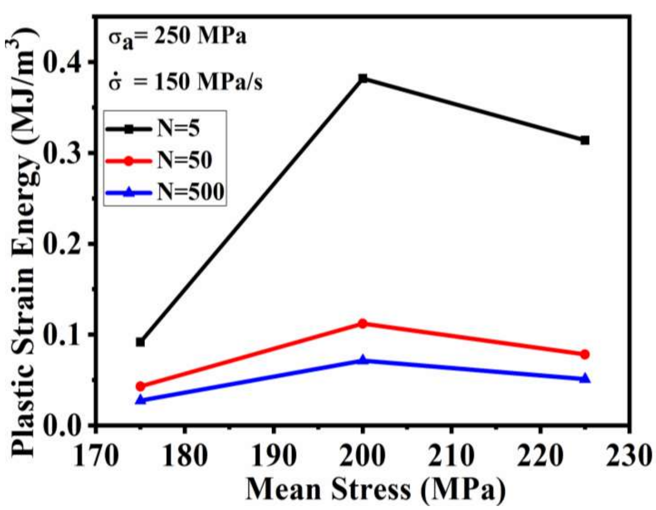

Fig. 4.13 Effect of mean stress on hysteresis loop energy of Inconel 617 alloy, at different number of cycles at constant stress amplitude of 250 MPa and stress rate of 150 MPa/s.

4.5.3 Impact of stress rate on stress-strain behaviour of Inconel 617 alloy under asymmetric cyclic stressing

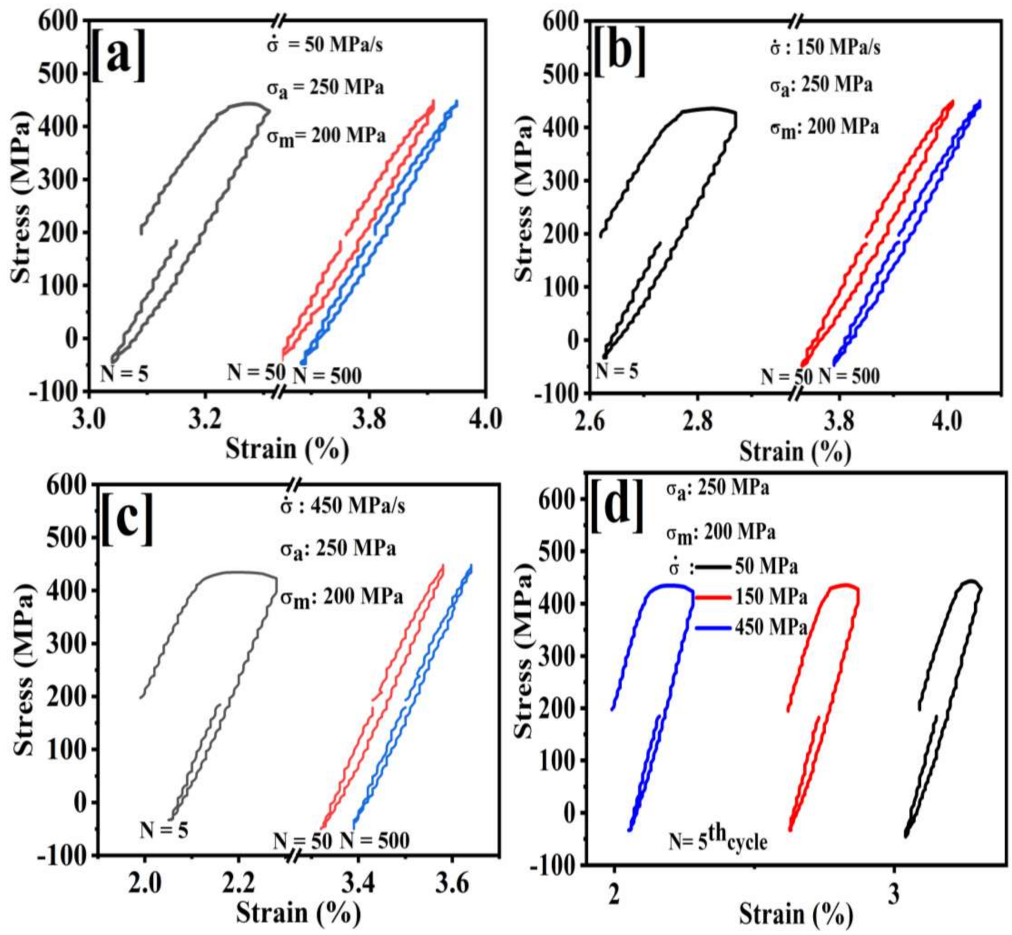

Fig. 4.14 Hysteresis loops of Inconel 617 alloy corresponding to 5, 50 and 500 stress cycles, at various stress rates: (a) 50 MPa/s, (b) 150 MPa/s, (c) 450 MPa/s, (d) comparison of width of 5th cycle loop at various stress rates, at constant stress amplitude of 250 MPa and mean stress of 200 MPa.

The impact of stress rate on the hysteresis loop at mean stress of 200 MPa and stress amplitude of 250 MPa is shown in Fig. 4.14. It may be observed from Figs. 4.14 (a, b and c) that with increase in stress rate the direction of accumulation of plastic strain moves in the lower strain direction. For a particular stress rate, with increase in the number of cycles, the width of hysteresis loop decreases, thereby increase in hardening of the material is reflected.

It can also be correlated with plastic strain energy plot (Fig. 4.15). Fig. 4.14 (d), in which the scale of strain is same for the tests carried out at the different stress rates, clearly shows that width of the hysteresis loops corresponding to 5^{th} cycle, increases with increase in stress rate. In the initial cycles, at higher stress rate larger number of dislocations are generated, due to which deformation is more and the width of the hysteresis loop is larger; however, with increase in cycles the width of the hysteresis loop decreases due to higher cyclic work hardening. Once the accumulated strain stabilizes, with increase in the stress rate, plastic strain energy decreases and shows cyclic hardening of the material (Fig. 4.15).

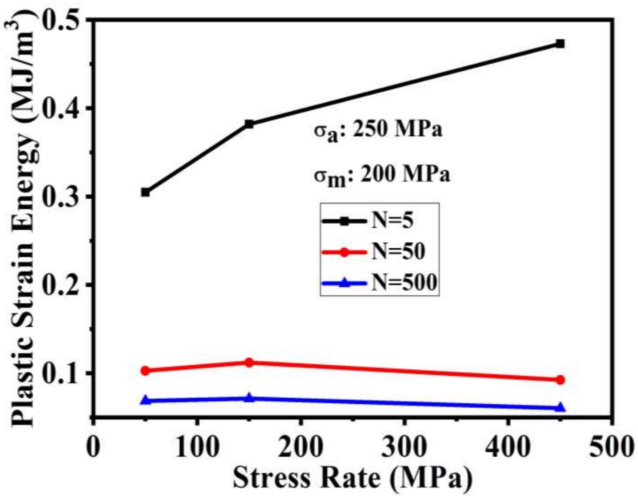

Fig. 4.15 Effect of stress rate on hysteresis loop energy of Inconel 617 alloy, at different number of cycles at constant stress amplitude of 250 MPa and mean stress of 200 MPa.

With increase in stress amplitude the maximum and minimum stresses increase and lead to more plastic deformation of the material. On the other hand, with increase in mean stress the tensile component of stress increases and compressive component decreases; hence, relatively less annihilation of dislocations occurs; and there is hardening of the material. Plastic strain energy per cycle decreases but overall ratcheting strain increases. In the case of stress rate, though the maximum and minimum stresses are constant but at higher stress rate there would be less effective annihilation of dislocations, which leads to hardening.

4.6 Fracture behaviour of Inconel 617 alloy

Inconel 617 alloy exhibited purely fatigue type of fracture under asymmetrical cyclic loading unlike the modified 9Cr-1Mo steel. The low magnification images under all the three parameters depicted flat type of fracture surface (Figs. 4.16a and c; Figs. 4.17a and c; Figs. 4.18a and c) comprising of both, some area showing fatigue signatures while other depicting tensile features. The higher magnified images from the region of fatigue failure exhibited striations, signifying purely fatigue features (Figs. 4.16b and d; Figs. 4.17b and d; Figs. 4.18b and d).

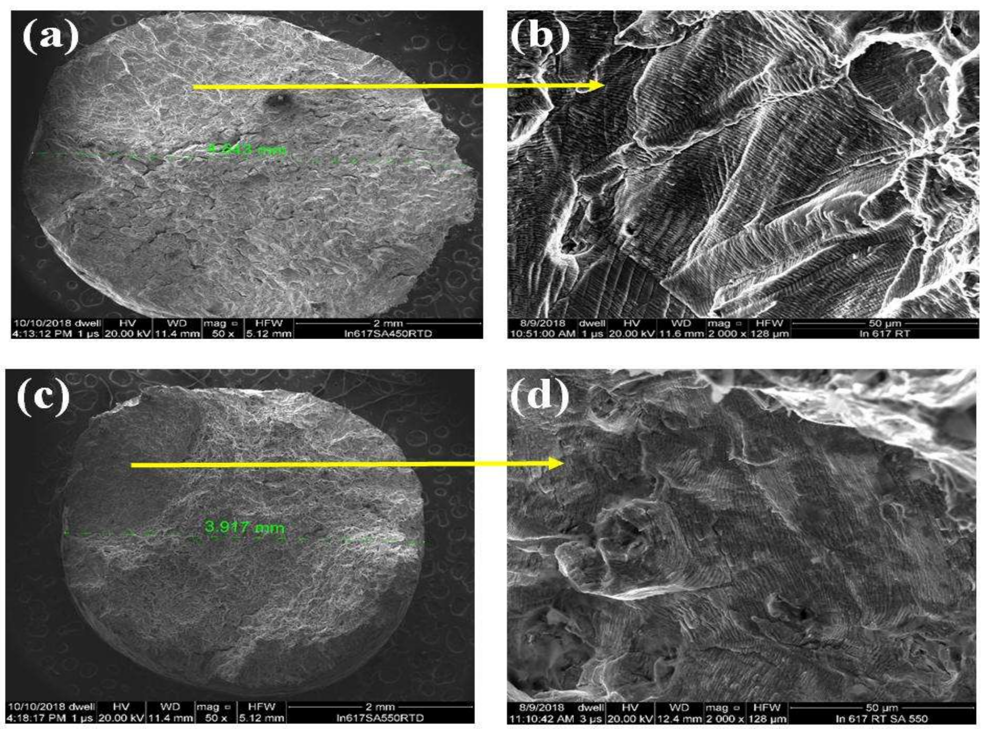

Fig. 4.16 Fracture behaviour of Inconel 617 alloy, showing the effect of stress amplitude at: (a and b) 450MPa (c and d) 550 MPa at constant mean stress of 200 MPa and stress rate of 150 MPa/s.

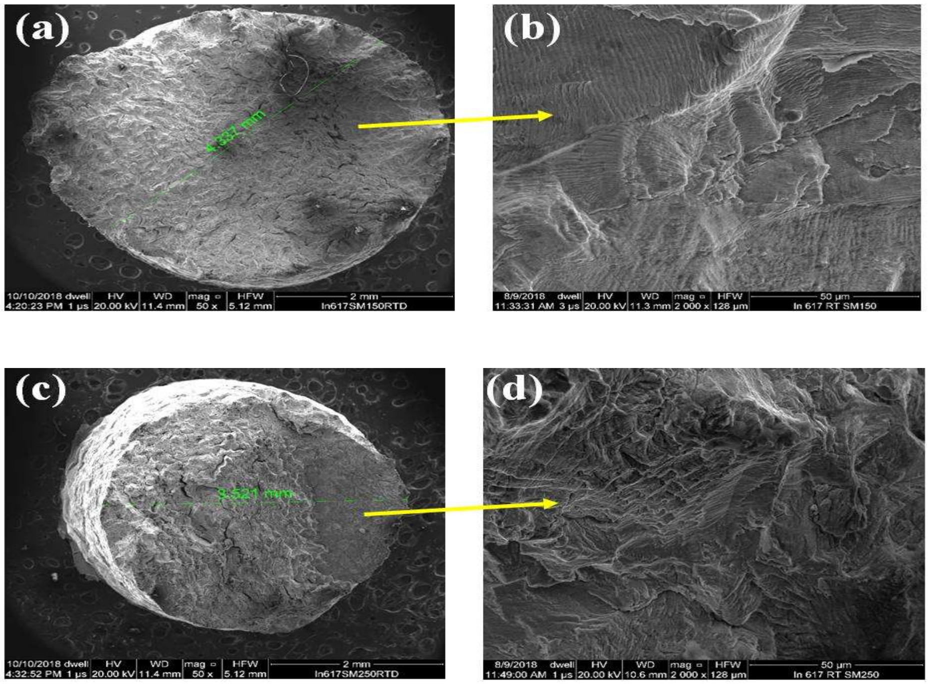

Fig. 4.17 Fracture behaviour of Inconel 617 alloy, showing the effect of mean stress at: (a and b) 150 MPa (c and d) 250 MPa at constant stress amplitude of 500 MPa and stress rate of 150 MPa/s.

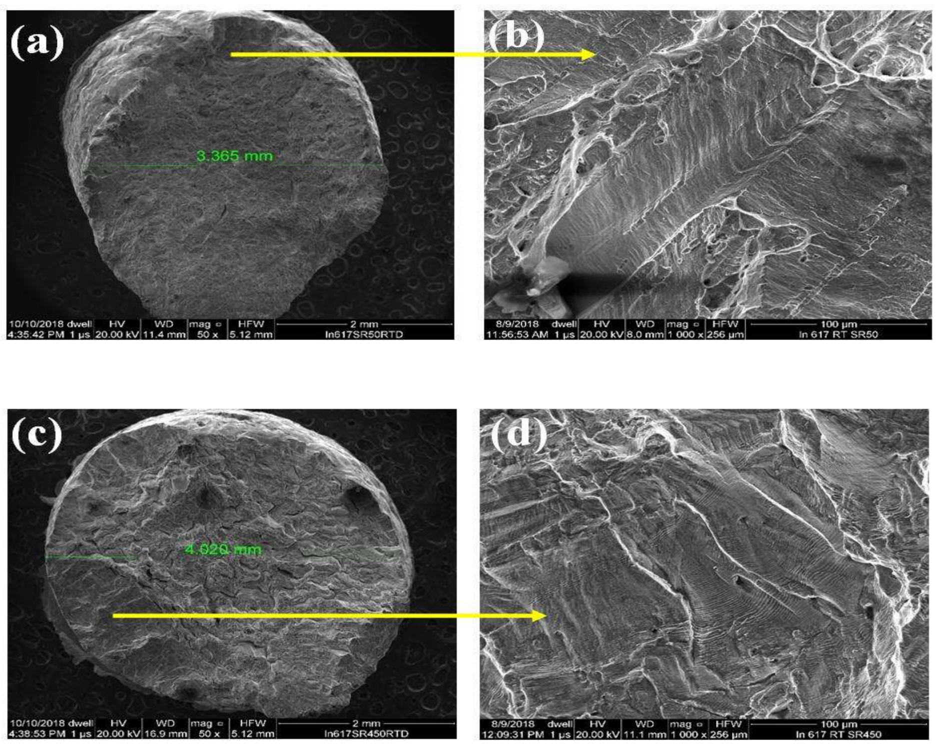

Fig. 4.18 Fracture behaviour of Inconel 617 alloy, showing the effect of stress rate at: (a and b) 50 MPa/s (c and d) 450 MPa/s at constant mean stress of 200 MPa and stress amplitude of 500 MPa.

4.7 Deformation behaviour of Inconel 617 alloy

The microstructure of the Inconel 617 alloy in solution treated condition showed single phase matrix, with dissolution of most of the precipitates, observed in the as-received condition. Deformation behaviour of this material under asymmetrical cyclic loading has been explained in detail under various parameters in discussion section of this chapter. The dislocation substructure has been explained with reference to dislocation density, formation of extended dislocations, bowing of dislocations and pinning of dislocations. At higher stress levels, due to heavy deformation, there is formation of persistent slip bands at regular intervals.

4.8 Comparison of uniaxial ratcheting behaviour of the alloys at room temperature

Ratcheting fatigue behaviour of modified 9Cr-1Mo steel and Inconel 617 alloy, tested under uniaxial sinusoidal loading with tensile mean stress at room temperature is compared in this section. For comparing ratcheting behaviour of these materials, mean stress and stress amplitude were normalized with respect to their ultimate tensile strengths.

Table 4.6 Ratcheting fatigue test matrix of the alloys, at RT at constant normalized stress amplitude of 0.58, normalized mean stress of 0.29 and stress rate of 150 MPa/s.

Material	Maximum stress σ_{max} (MPa)	Minimum stress σ_{min} (MPa)	Stress Amplitude σ_a (MPa)	Mean stress σ_m (MPa)	Normalized stress amplitude (σ_a / σ_{UTS})	Normalized mean stress (σ_m / σ_{UTS})	No. of cycles to failure (N_f)
Modified 9Cr-1Mo steel	620	-200	410	210	410/713= 0.58	210/713=0.29	1506
Inconel 617 alloy	730	-240	485	245	500/835=0.58	250/835=0.29	4206

Fatigue tests were conducted keeping normalized mean stress and normalized stress amplitude, identical for both materials [Rajpurohit et al., (2021); Kang et al., (2011)]. Data for fatigue life of materials, corresponding to normalized mean stress and stress amplitude are presented in Table 4.6. It may be seen from Table 4.6 that fatigue life under identical normalized mean stress and stress amplitude is higher for Inconel 617 alloy in comparison with the life of modified 9Cr-1Mo steel.

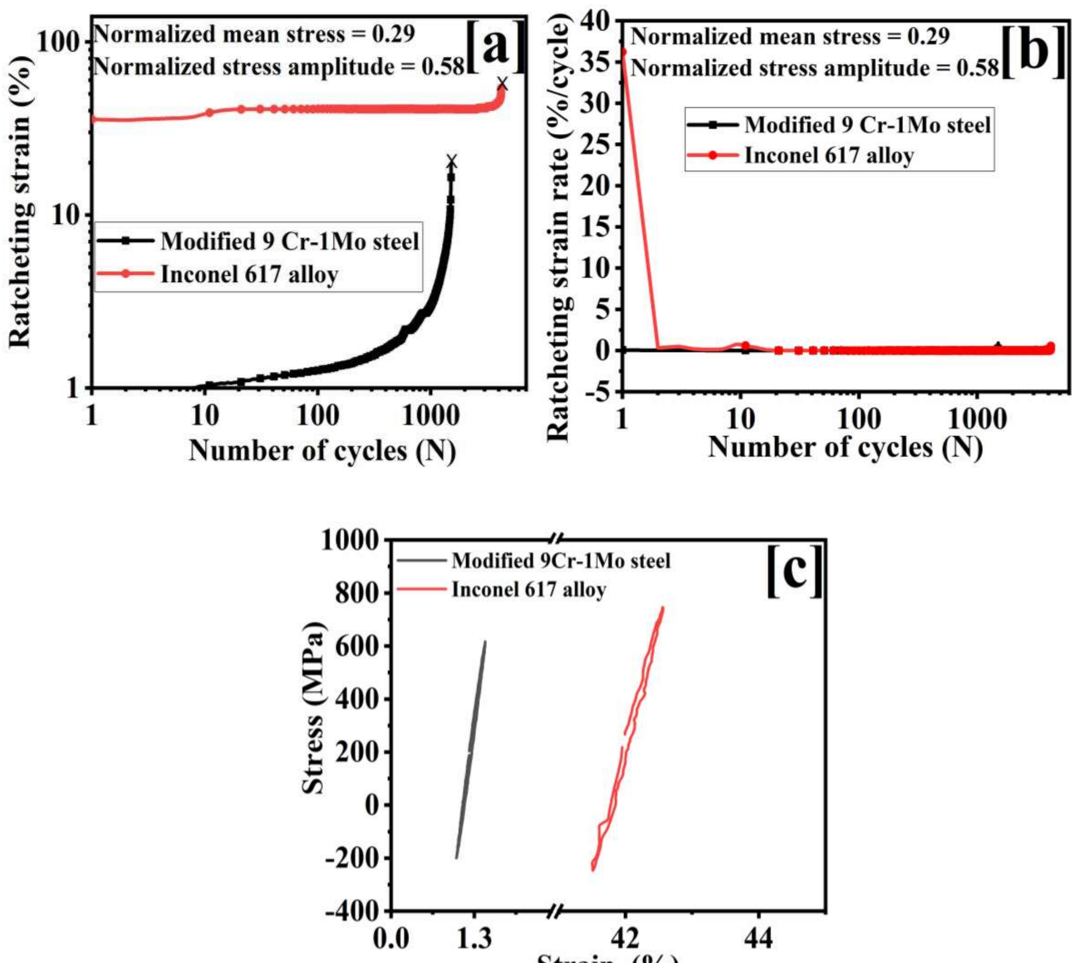

Fig. 4.19 (a) Cumulative ratcheting strain vs number of cycles (b) ratcheting strain rate and (c) hysteresis loops corresponding to 20th cycle of modified 9Cr-1 Mo steel and Inconel 617 alloy.

Ratcheting strain accumulation (Fig. 4.19a) in Inconel 617 alloy is significantly higher than that in modified 9Cr-1Mo steel. Similarly, rate of ratcheting strain evolution shown in Fig. 4.19(b) is significantly higher in Inconel 617 alloy than that in modified 9Cr-1Mo steel, up to about 20 initial cycles; however, later it becomes stabilized and almost equals that of modified steel. Width as well as area of hysteresis loop of the 20th cycle is larger of the Inconel 617 alloy than that of modified steel (Fig. 4.19c), due to higher accumulation of plastic strain in Inconel 617 alloy.

4.9 Discussion

4.9.1 Ratcheting fatigue behaviour of Inconel 617 alloy

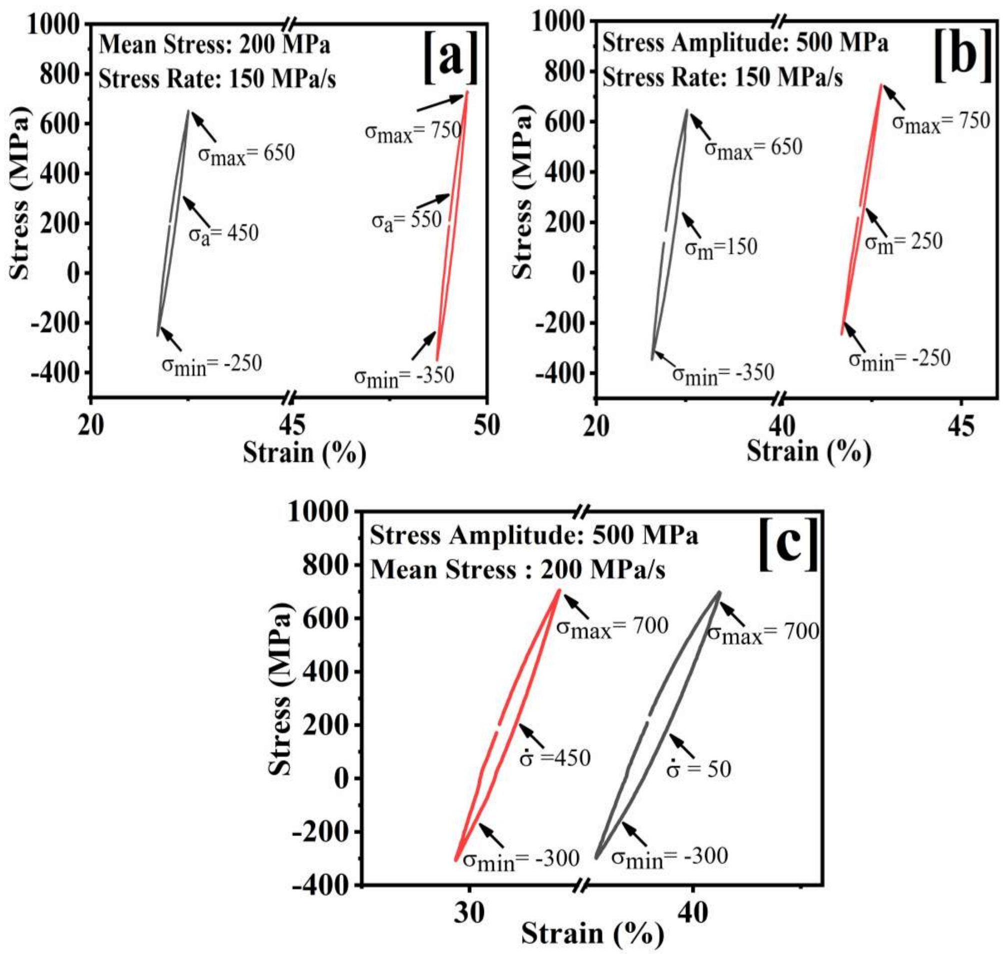

Fig. 4.20 Variation in the 20th cycle hysteresis loops of Inconel 617 alloy, due to increase in: (a) stress amplitude from 450 to 550 MPa, (b) mean stress from 150 to 250 MPa and (c) stress rate from 50 to 450 MPa/s.

The influence of stress amplitude on cyclic life, in comparison with the other variables, was found relatively more significant. The loops of hysteresis corresponding to 20^{th} cycle of the samples, tested at the various stress amplitudes of 450 to 550 MPa, at a constant mean stress of 200 MPa and the stress rate of 150 MPa/s were analysed. The reduction in cyclic life with increase in ratcheting strain, with increase in stress amplitude, is in line with earlier observations [Rajpurohit et al., (2018)]. With increase in stress amplitude, the width and area of hysteresis loops increased, as displayed in Fig. 4.20(a) and the effect of stress amplitude on fatigue life can also be correlated with the plastic strain energy plot (Fig. 4.21a). There was increase in maximum and minimum stresses with rise in amplitude, due to which plastic strain range increased and the fatigue life was lowered.

Microstructure of the specimens, tested at the lowest stress amplitude of 450 MPa showed banding and also bowing of dislocations (shown by arrows) as shown in Fig. 4.22(a). The micrograph in Fig. 4.22(b) displays pinning of dislocations by fine carbide precipitates, the magnified image in the inset shows the pinning, more clearly. At the highest stress amplitude of 550 MPa, the number of persistent slip bands increased and there was decrease in the width of slip bands (Fig. 4.22c); also, the dislocation density increased (Fig. 4.22d). With increase in the stress amplitude, the number of slip bands increased due to activation of more slip systems, due to which plastic strain increased and cyclic life was reduced.

Fracture characteristics of the specimens, tested under asymmetric cyclic loading, showed distinct fatigue striations. Figs. 4.16(a and c) show low magnification fractographs of the samples tested at the lowest and highest stress amplitudes of 450 and 550 MPa respectively. The region of the fracture surface resulting from fatigue has been magnified and distinct fatigue striations may be observed in Figs. 4.16(b and d) for the stress amplitudes referred to above. There was formation of distinct neck in the sample tested at the highest stress amplitude of 600 MPa.

There is reduction in ratcheting fatigue life with increase in the stress amplitude; as stress amplitude is increased from 450 MPa to 500 MPa, fatigue life is decreased by 35.7%, when stress amplitude is increased from 500 MPa to 550 MPa fatigue life is reduced by 65.1% with respect to that at 500 MPa but with increase in stress amplitude from 550 MPa to 600 MPa fatigue life is decreased by 98.6% of that at 550 MPa.

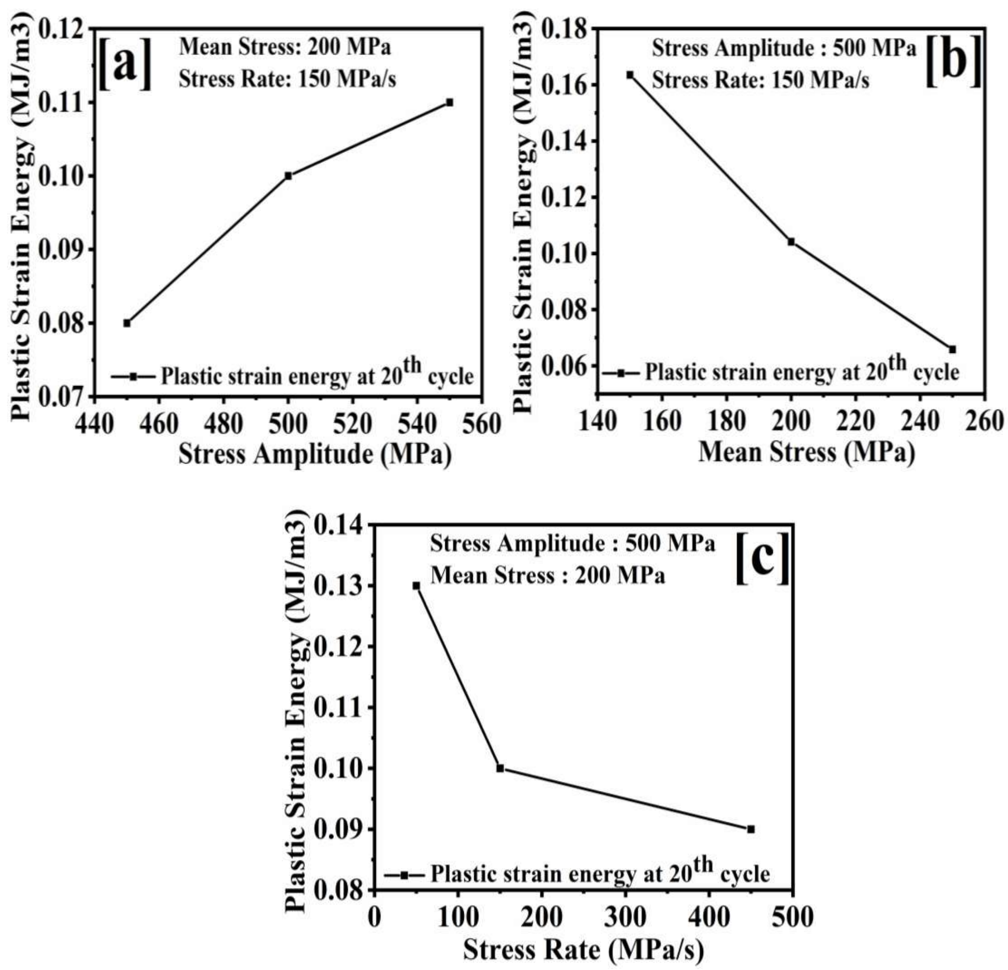

Fig. 4.21 Variation in plastic strain energy at the 20th cycle of Inconel 617 alloy, due toincrease in:(a) stress amplitude from 450 to 550 MPa, (b) mean stress from 150 to 250 MPa and (c) stress rate from 50 to 450 MPa/s.

Ratcheting strain was 73% in the sample tested at stress amplitude of 600 MPa, and that is much higher than the uniform strain of 54%; therefore, there was necking and fatigue life was reduced drastically. Occurrence of necking in fatigue sample, tested at the highest stress amplitude of 600 MPa and corresponding maximum stress of 800 MPa, in spite of maximum stress being less than UTS (835 MPa) may be due to localised decrease in cross sectional area under dynamic loading.

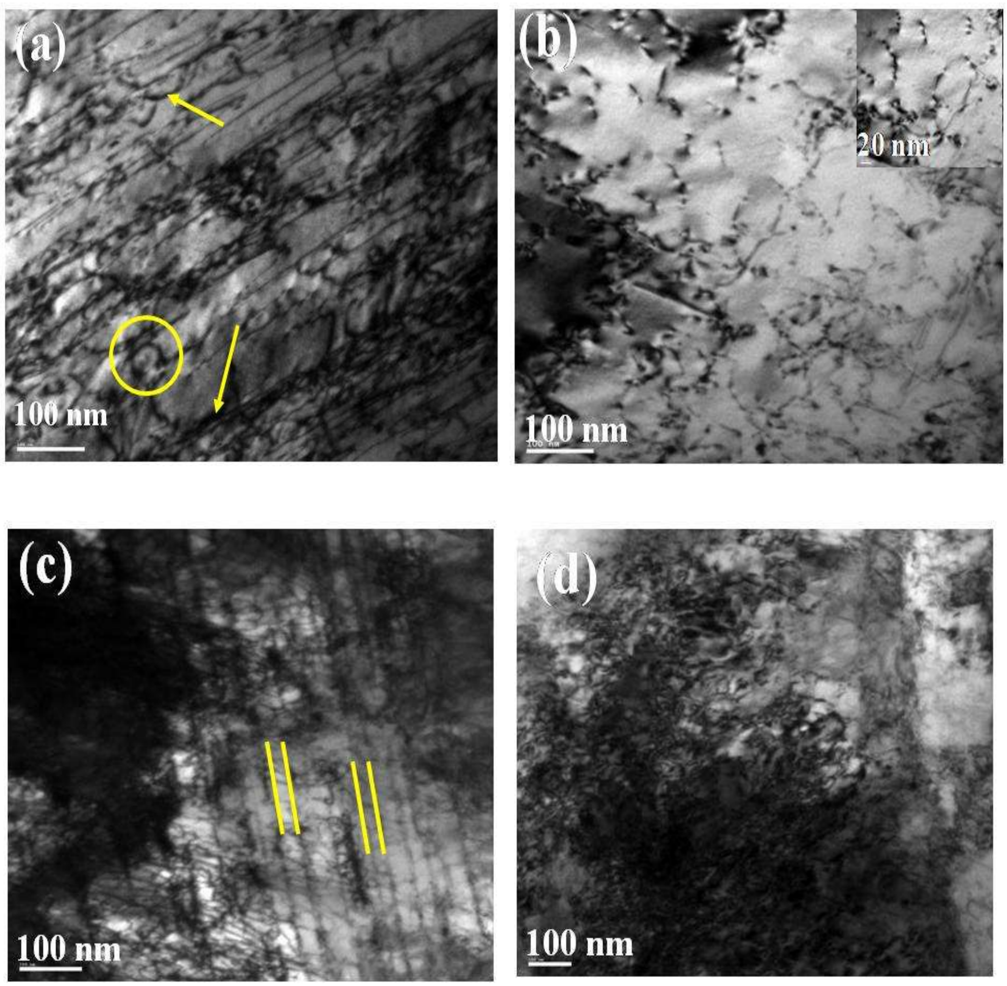

Fig. 4.22 Bright field TEM micrographs of Inconel 617 alloy, showing the effect of stress amplitude at: (a and b) 450 MPa (c and d) 550 MPa, tested at constant mean stress of 200 MPa and stress rate of 150 MPa/s.

For better visualisation of the impact of mean stress on ratcheting behaviour of the Inconel 617 alloy, several loops were recorded at different cycles and were analysed. The 20th cycle stress- strain hysteresis loop was used for comparison, as the strain induced in tension and compression was stabilized up to 20 cycles. It was observed that with increase in the mean stress from 150 to 250 MPa, the loops shifted towards tension side and maximum stress increased from 650 to 750 MPa (Fig. 4.20b), likewise the degree of work hardening increased.

One important point to notice is that with increase in tensile mean stress, the area of hysteresis loops as well as width of loops decreased (Fig. 4.20b), due to higher degree of wok hardening, from increase in the maximum stress and this can also be visualized from plastic strain energy plot (Fig. 4.21b). Due to increase in the mean stress, plastic strain energy decreased, and that resulted in hardening of the material. The decrease in plastic strain energy with increase in mean stress is due to increase in the maximum stress and consequent increase in work hardening of the material. Therefore, the plastic strain energy decreased for that particular cycle as compared to that at the lower mean stress. However, due to continuous loading and higher maximum stress, the total ratcheting strain was more in comparison with that at lower mean stress.

During cyclic loading, generation and annihilation of dislocations take place. As mentioned above, with increase in mean stress the hysteresis loops shifted towards tension side and the magnitude of the minimum stress (σ_{min}) decreased, suggesting that annihilation of dislocations remained incomplete which led to increase in remnant dislocation density [Rajpurohit et al.,(2018)]. It may be observed from the TEM micrographs that at the lowest mean stress of 150 MPa, there are persistent slip bands, shown by lines in Fig. 4.23(a), and there is pinning of dislocations, as shown by arrow in

Fig. 4.23(b). In contrast, at the maximum mean stress of 250 MPa, the width of bands increased (Fig. 4.23c) and also the dislocation density increased (Fig. 4.23d).

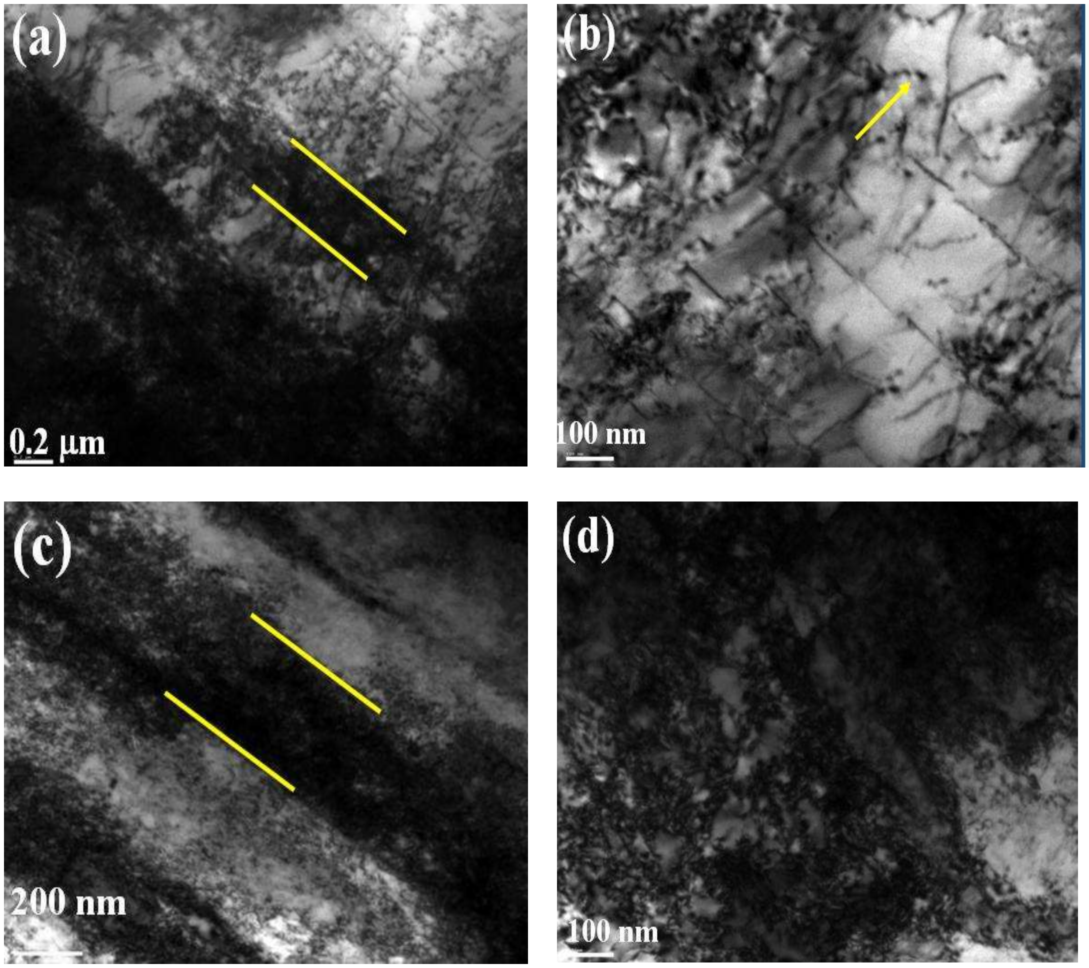

Fig. 4.23 Bright field TEM micrographs of Inconel 617 alloy, showing the effect of mean stress at: (a and b) 150 MPa (c and d) 250 MPa, tested at constant stress amplitude of 500 MPa and stress rate of 150 MPa/s.

Fractographs of the samples, tested under asymmetric cyclic loading at different mean stresses show fatigue striations. Figs. 4.17 (a and c) show low magnification images of the fracture of the samples tested at the lowest and highest mean stress of 150 and 250 MPa respectively, and the regions of the fracture surfaces, resulting from fatigue are magnified in Figs. 4.17 (b and d). It is evident that the region of fatigue fracture of the sample, tested at the lowest mean stress of 150 MPa is smooth and there are distinct fatigue striations (Fig. 4.17b) whereas that of the sample tested at the highest mean stress of 250 MPa is quite rough and the striations are less obvious (Fig. 4.17d). It is due to higher degree of work hardening of the material at the higher mean stress of 250 MPa that would have enhanced the process of fatigue crack initiation and propagation, leading to decrement in fatigue life. The nature of hardening and softening depends on other factors like uniform plastic strain, degree of work hardening, and resistance of material against fatigue crack initiation and prapogation.

The impact of stress rate on the cyclic hysteresis loops is depicted in Fig. 4.20(c). It is clear from Figs. 4.9(a,b) that the accumulation as well the rate of accumulation of ratcheting strain decreases with increase in stress rate from 50 to 450 MPa/s and the cyclic life increases. Due to increase in the stress rate, the area and width of the hysteresis loop decreased, thereby plastic strain accumulation decreased and cyclic life increased. It is clearly seen from the plastic strain energy plot (Fig. 4.21c) that with increase in stress rate, plastic strain energy is decreased, and that resulted in hardening of the material.

This behaviour may be due to less effective annihilation of dislocations generated during the tensile and compressive load cycles and consequent increase in number of dislocations and thereby in work hardening, with increase in the stress rate. It can be very well correlated with TEM micrographs which show increase in number of dislocations with increase in stress rate from 50 MPa/s (Fig. 4.24a) to 450 MPa/s (Fig. 4.24b).

The fracture features of the sample tested at the lowest stress rate of 50 MPa/s are depicted in Figs. 4.18 (a and c). It can be observed from the fractographs that the sample tested at the highest stress rate of 450 MPa/s, lasted for more cycles, as seen from the much larger number of striations and much smaller inter striation spacing (Fig. 4.18d) than that of the sample tested at the lower stress rate of 50 MPa/s (Fig. 4.18b).

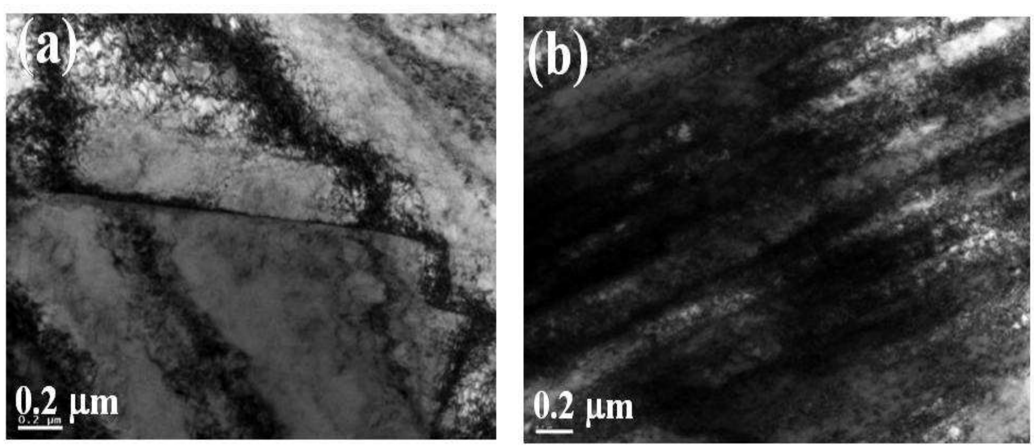

Fig. 4.24 Bright field TEM micrographs of Inconel 617 alloy, showing the effect of stress rate on dislocation substructure, tested at constant stress amplitude of 450 MPa and mean stress of 200 MPa, at: (a) 50 MPa/s (b) 450 MPa/s.

4.9.2 Comparison of uniaxial ratcheting behaviour of the alloys at room temperature

The microstructures of both the materials as reported earlier [Rao et al., (2019); Verma et al., (2016)] contain carbides. These are distributed in laths, along lath boundaries and also grain boundaries in modified 9Cr-1Mo steel, whereas carbides are associated with austenite grain boundaries in Inconel 617 alloy. It is evident from Figs. 4.19(a and b) that accumulation of ratcheting strain was much higher in Inconel 617 alloy than that in modified 9Cr-1Mo steel, at normalized mean stress of 0.29 and normalized stress amplitude of 0.58.

Also, hysteresis loops of 20th cycle of two materials (Fig. 4.19 c) clearly show that plastic strain accumulation in Inconel 617 alloy is more than that in modified 9Cr-1Mo steel, as width and area of the hysteresis loop is more in Inconel 617 alloy. It is important to point out that though accumulation of ratcheting strain is much higher in Inconel 617 alloy, still it exhibits higher fatigue life as compared to the life depicted by modified 9Cr-1Mo steel. The reason for observed behaviour is that in Inconel 617 alloy, the degree of work hardening is much higher (2.41), in comparison with that of modified 9Cr-1Mo steel (1.24).

It may be seen from Table 4.1 that uniform plastic strain in Inconel 617 alloy is much higher (nearly by seven times) than that of modified 9Cr-1Mo steel. It may be noted from Fig. 4.19(a) that cumulative ratcheting strain in the Inconel 617 alloy is 52% and that in modified 9Cr-1Mo steel is 20%, even then, the modified 9Cr-1Mo steel sample fractured in much smaller number of cycles (1506) than that of the Inconel 617 alloy (4206).

It was due to the fact that uniform plastic strain in the modified 9Cr-1Mo steel was only 8%; hence, once cumulative ratcheting strain exceeded 8% (the uniform plastic strain), there was onset of necking, that caused rapid reduction in load bearing capacity of the material and led to rapid fracture in tensile mode (Fig. 4.25a).On the other hand, though the cumulative ratcheting strain in Inconel 617 alloy was much higher (52%), it did not exceed the uniform plastic strain of 54%; therefore, necking did not occur and the failure occurred by usual process of fatigue, through crack initiation and propagation, as depicted in Figs. 4.25(b and d). The change in orientation of striations across certain lines in Fig. 4.25(d) is due to fatigue crack propagation on differently oriented crystallographic planes in different grains.

Excessive plastic deformation, exceeding the degree of work hardening of the material, would increase the tendency for fatigue crack initiation and propagation, however, the degree of work hardening would accommodate the accumulating plastic strain resulting from ratcheting and would not allow onset of necking, and the fatigue life will be enhanced. Low uniform plastic strain, resulting from low degree of work hardening, would cause necking and thereby reduction in fatigue life.

Tapered annular region, surrounding central region of tensile fracture in Fig. 4.25(a), clearly shows occurrence of necking in modified 9Cr-1Mo steel; in sharp contrast, there is no necking in Inconel 617 alloy (Fig. 4.25b).

It may thus be seen that in respect of ductility parameter, elongation to fracture, uniform elongation plays major role on ratcheting fatigue life. Dimples on fracture surface of the modified 9Cr-1Mo steel (Fig. 4.25c) occurred essentially due to necking that led to tensile fracture.

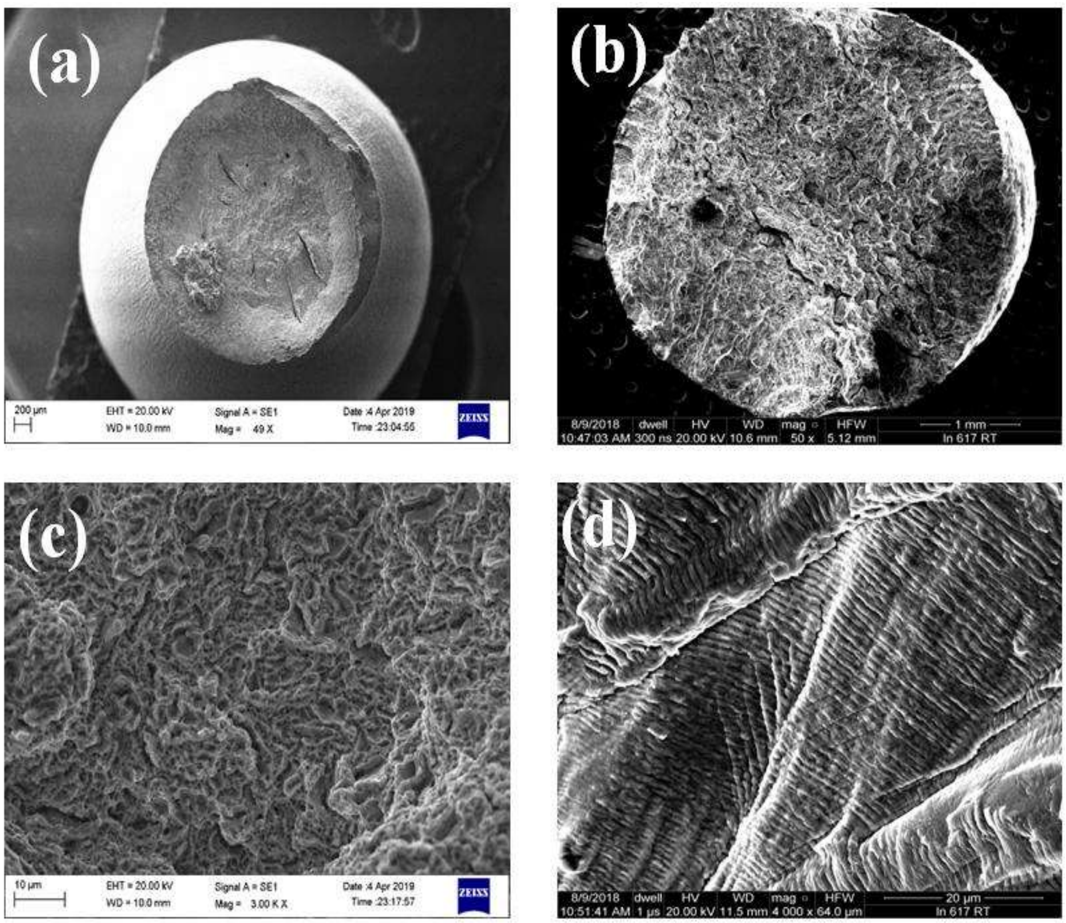

Fig. 4.25 Fractographs of both alloys tested under ratcheting: (a and c) modified 9Cr-1Mo steel, (b and d) Inconel 617 alloy.

4.10 Summary

The important observations of ratcheting behaviour of Inconel 617 alloy at room temperature are listed below:

1. The permanent strain and its rate increase with mean stress and stress amplitude whereas both of these decrease with increase in stress rate.

2. With rise in stress amplitude, cyclic life decreases. At lower stress amplitude, there is formation of slip bands and pinning of dislocations by carbide particles, whereas at higher stress amplitude, there is formation of more slip bands at regular intervals.
3. Plastic strain accumulation increases with mean stress and fatigue life is reduced and dislocation density is increased with mean stress.
4. Accumulation of permanent strain is reduced with increase in stress rate and fatigue life is increased under asymmetric cyclic loading.
5. On comparing the ratcheting behaviour of the alloys at ambient temperature, Inconel 617 alloy showed higher fatigue life in comparison with that of the modified 9Cr-1Mo steel. The reason behind this is higher uniform elongation value (54%) for Inconel 617 alloy. Thus, uniform strain can be considered as an important tensile parameter for selection of materials for piping and tubing components, experiencing ratcheting fatigue.